

Sustainable Photoredox C(sp³)–P Bond Formation via Nitrogen-Vacancy-Engineered Carbon Nitride

Barbaros Bolat^a, Melek Sermin Ozer^a, Kang Sun^b, Hai-Long Jiang^b, Zafer Eroglu^{a*}, and Onder Metin^{ac*}

^aDepartment of Chemistry, College of Sciences, Koç University, 34450 Istanbul, Türkiye

^bHefei National Research Center for Physical Sciences at the Microscale, Department of Chemistry, University of Science and Technology of China, 230026 Hefei, People's Republic of China

^cKoç University Surface Science and Technology Center (KUYTAM), 34450 Istanbul, Türkiye

*To whom should be corresponded: Dr. Zafer Eroğlu, email: zeroglu@ku.edu.tr, Prof. Ö. Metin, email: ometin@ku.edu.tr

Table of Contents

Abbreviations	4
Experimental Section	5
Chemicals	5
Characterization Instruments	5
Synthesis of Tertiary Amines	6
Characterization of Materials	7
NMR Results	25
NMR Spectra	28
References	34

List of Figures

Figure S1. The XRD patterns of pristine and annealed CN derivatives using the precursor a) cyanamide, b) dicyandiamide, and c) melamine.	7
Figure S2. The FT-IR spectra of pristine and annealed CN derivatives using the precursor a) cyanamide, b) dicyandiamide, and c) melamine.	8
Figure S3. The XPS survey spectra of pristine and annealed CN derivatives using the precursor a) cyanamide, b) dicyandiamide, and c) melamine.	9
Figure S4. The high resolutions C 1s a-c) and N 1s d-f) XPS spectra of pristine and annealed CN derivatives using the precursor cyanamide, dicyandiamide, and melamine.	10
Figure S5. SEM images of a and b) CN(D), c and d) <i>Nv</i> -CN(D)600N ₂ , e and f) CN(M), g and h) <i>Nv</i> -CN(M)650Ar at different magnification.	12
Figure S6. The Brunauer–Emmett–Teller (BET) N ₂ adsorption/desorption isotherms of pristine and annealed CN derivatives using the precursor a) cyanamide, b) dicyandiamide, and c) melamine.	13
Figure S7. The UV-Vis absorption spectra of pristine and annealed CN derivatives using the precursor a) cyanamide, b) dicyandiamide, and c) melamine.	14
Figure S8. The Tauc plots of pristine and annealed CN derivatives using the precursor a) cyanamide, b) dicyandiamide, and c) melamine.	15
Figure S9. The PL spectra of pristine and annealed CN derivatives using the precursor a) cyanamide, b) dicyandiamide, and c) melamine.	16
Figure S10. ¹ H NMR of compound 5 a) pure, b) reaction time is 2 h and c) reaction time is 5 h (control experiments showing the possible degradation of compound 5 for longer period of reaction. Note* ¹ H NMR in b) and c) contain internal standard 1,3-dinitrobenzene).	17
Figure S11. GC-MS of byproducts (compound 5 after treating under optimized conditions with longer duration).	17
Figure S12. a) The reusability trials for ten consecutive cycles, b) The XPS survey spectra, The high resolutions c) C 1s and d) N 1s XPS spectra, e) The XRD pattern, and f) The FT-IR spectra of <i>Nv</i> -CN(C)-650Ar before and after use in ten consecutive cycles.	23
Figure S13. The TEM image of photocatalyst <i>Nv</i> -CN(C)-650Ar after a-b) five consecutive cycles of, and c-d) ten consecutive cycles of reusability experiments.	24
Figure S14. ¹ H NMR of compound 3 (CDCl ₃).	28

Figure S15. ^{13}C NMR of compound 3 (CDCl_3).....	28
Figure S16. ^1H NMR of compound 5 (CDCl_3).....	29
Figure S17. ^{13}C NMR of compound 5 (CDCl_3).....	29
Figure S18. ^1H NMR of compound 7 (CDCl_3).....	30
Figure S19. ^{13}C NMR of compound 7 (CDCl_3).....	30
Figure S20. ^1H NMR of compound 11 (CDCl_3).....	31
Figure S21. ^{13}C NMR of compound 11 (CDCl_3).....	31
Figure S22. ^1H NMR of compound 13 (CDCl_3).....	32
Figure S23. ^{13}C NMR of compound 13 (CDCl_3).....	32
Figure S24. ^1H NMR of compound 15 (CDCl_3).....	33
Figure S25. ^{13}C NMR of compound 15 (CDCl_3).....	33

List of Tables

Table S1. Calculated $\text{C}=\text{N}/-\text{NH}_x$ ratios of pristine and annealed CN derivatives by XPS peak area analysis.....	10
Table S2. Organic elemental composition (CHN) analysis of pristine and annealed CN derivatives.....	11
Table S3. Optimization table for the model reaction.....	18

Abbreviations

BQ: p-benzoquinone

CB: Conduction Band

CN: Carbon nitride

CP MAS NMR: Cross-polarization magic angle spinning nuclear magnetic resonance

DCM: Dichloromethane

DMF: Dimethylformamide

DMSO: Dimethyl Sulfoxide

DOPO: 9,10-dihydro-9-oxa-10-phosphaphenanthrene-10-oxide

EIS: Electrochemical impedance spectroscopy

EPR: Electron paramagnetic resonance

EtOAc: Ethyl Acetate

FT-IR: Fourier-transform infrared spectroscopy

HAT: Hydrogen-atom transfer

ICP-MS: Inductively coupled plasma mass spectroscopy

IPA: Isopropanol

MeCN: Acetonitrile

NHE: Normal hydrogen electrode

Nv: Nitrogen vacancy

Nv-CN(X)-TG: Nitrogen vacant Carbon nitride synthesized from **X** precursor, annealed at **T** temperature under **G** atmosphere.

Nv-CN: Nitrogen vacant Carbon nitride

PL: Photoluminescence

SEM: Scanning electron microscopy

SET: Single-electron transfer

TEM: Transmission electron microscopy

TEMPO: 2,2,6,6-tetramethylpiperidine-1-oxyl

TEOA: Triethanolamine

THF: Tetrahydrofuran

TPC: Transient photocurrent

TRPL: Time-resolved photoluminescence

UV-Vis DRS: Ultraviolet-visible diffuse reflectance spectroscopy

VB: Valance Band

XPS: X-ray photoelectron spectroscopy

XRD: X-Ray Diffraction

Experimental Section

Chemicals

Cyanamide ($\geq 98\%$, Sigma-Aldrich), Dicyandiamide ($\geq 99\%$, Sigma-Aldrich), Melamine ($\geq 99\%$, Sigma-Aldrich), Copper (I) iodide ($\geq 98\%$, Sigma-Aldrich), Potassium phosphate tribasic ($\geq 98\%$, Sigma-Aldrich), Ethylene glycol ($\geq 99\%$, Sigma-Aldrich), isopropanol ($\geq 99.5\%$, IsoLab), 1,2,3,4-Tetrahydroisoquinoline ($\geq 95\%$, Sigma-Aldrich), 4-iodoacetophenone ($\geq 97\%$, Sigma-Aldrich), Acetonitrile ($\geq 99\%$, IsoLab), Ethyl Acetate ($\geq 99\%$, IsoLab), Cyclohexane ($\geq 99\%$, IsoLab), Ethanol ($\geq 99\%$, IsoLab), Toluene ($\geq 99\%$, IsoLab), Dimethyl sulfoxide ($\geq 99\%$, IsoLab), dimethyl formamide ($\geq 99\%$, IsoLab), tetrahydrofuran ($\geq 99\%$, IsoLab), 9,10-dihydro-9-oxa-10-phosphaphenanthrene-10-oxide ($\geq 99\%$, Sigma-Aldrich), p-Benzoquinone ($\geq 98\%$, Sigma-Aldrich), 2,2,6,6-tetramethylpiperidine-1-oxyl ($\geq 99\%$, Sigma-Aldrich), Triethanolamine ($\geq 99\%$, Sigma-Aldrich), Silver nitrate ($\geq 99\%$, Sigma-Aldrich), Sodium Azide ($\geq 99.5\%$, Chem Solute), Diethyl phosphite ($\geq 99\%$, Sigma-Aldrich), Dibutyl phosphite ($\geq 99\%$, Sigma-Aldrich), Diphenyl phosphite ($\geq 99\%$, Sigma-Aldrich), Iodobenzene ($\geq 99\%$, Sigma-Aldrich), 4-iodotoluene ($\geq 99\%$, Sigma-Aldrich), Piperidine ($\geq 99\%$, Sigma-Aldrich), 1,3-dinitrobenzene (97% , Sigma-Aldrich), Chloroform-d (99.8% , Sigma-Aldrich). Except as otherwise specified, all compounds and solvents were utilized without additional purification.

Characterization Instruments

The X-ray diffraction (XRD) measurements were performed by Bruker D2 Phaser X-ray diffractometer using Cu K α radiation (1.54 Å). X-ray photoelectron spectroscopy (XPS) was carried out by Thermo K-Alpha XPS using Al K α radiation (1486.6 eV). The Fourier-transform infrared spectroscopy (FT-IR) analyses were conducted by Thermo Scientific iS 10 FT-IR Spectrometer with ATR module. CHN elemental analyses were executed by Thermo Scientific Flash 2000. The diffuse reflectance spectroscopy (DRS) analyses were implemented by Shimadzu UV-3600 UV-vis-NIR spectrophotometer. Photoluminescence (PL) spectroscopy analyses were employed by Agilent Cary Eclipse PL at 320 nm. The nuclear magnetic resonance (NMR) analyses were performed by Bruker 500 MHz Ascend NMR spectrometer. NMR spectra were obtained in CDCl₃ using tetramethylsilane (TMS) as the internal standard. While chemical shifts are reported in parts per million (ppm), coupling constants (J values) are reported in Hz. The Bruker TopSpin 4.2.0 application was used to process the NMR spectra. For ssNMR analysis of ¹³C, Bruker 500 MHz Ascend Neo NMR spectroscopy with MASSBDR-BBLR CPMAS H/X VTN 4 mm double resonance probe for SB solid state was used.

Electron paramagnetic resonance (EPR) measurements were conducted on CIQTEK EPR200M with continuous-wave X band frequency, where methanol was used as solvent and before recording radical signals, all samples were irradiated under light for 1 min. The Brunauer–Emmett–Teller (BET) measurements were employed on a Micromeritics Accelerated Surface Area and Porosimetry System ASAP 2020 HD (−195.804 °C). The electrochemical measurements were conducted on a CHI 660E electrochemical workstation using Hg/Hg₂Cl₂ reference and Pt wire counter electrodes. Prior to the measurements, 2.50 mg of CN(X) and *N*-CN(X)-TG derivatives were sonicated in 5 mL ethanol and spray coated on a 1 cm² area on ITO glasses to produce working electrodes. The measurements were performed in 0.1 M Na₂SO₄ solution. The Mott-Schottky analyses were employed at 1, 1.5, and 2 kHz with a potential range of −1.2 to 1.0 V. The EIS analyses were conducted at 1 V potential with the frequency range of 0.01 Hz to 100 kHz for the Nyquist plots. The inductively coupled plasma mass spectrometry (ICP-MS) analyses were conducted on an Agilent 7800 system (Agilent Technologies, Waldbronn, Germany).

Synthesis of Tertiary Amines

N-(4-acetylphenyl)-tetrahydroisoquinoline (**1**) was synthesized by a validated method.¹ In a 100-mL round bottom flask, 200 mg of copper(I) iodide (1.05 mmol, 10 mol%), 4.25 g of tribasic potassium phosphate (20 mmol, 2 equivalent), and 2.46 g of 4-iodoacetophenone (10 mmol, 10 equivalent) were put. The flask was first vacuumed and then filled with Ar gas. 20 mL of isopropanol, 1.1 mL of ethylene glycol (20.00 mmol, 2 equivalent), and 2.0 mL of 1,2,3,4-tetrahydroisoquinoline (15 mmol, 1.5 equivalent) were added. The mixture was heated at around 90°C for 24 hours under stirring. After the heating was stopped, the reaction mixture was allowed to cool to room temperature, filtered and 20 mL of DCM and 20 mL of water were added to the filtrate. The organic layer was extracted three times with DCM and collected organic phase was dried over anhydrous sodium sulfate. Compound **1** was purified from the organic phase by column chromatography on silica with cyclohexane/ethyl acetate eluent with 6:1 ratio. The compound was crystallized as yellow needles and verified by ¹H-NMR. Compounds **4**, **6**, and **8** were synthesized with the same methodology.

Characterization of Materials

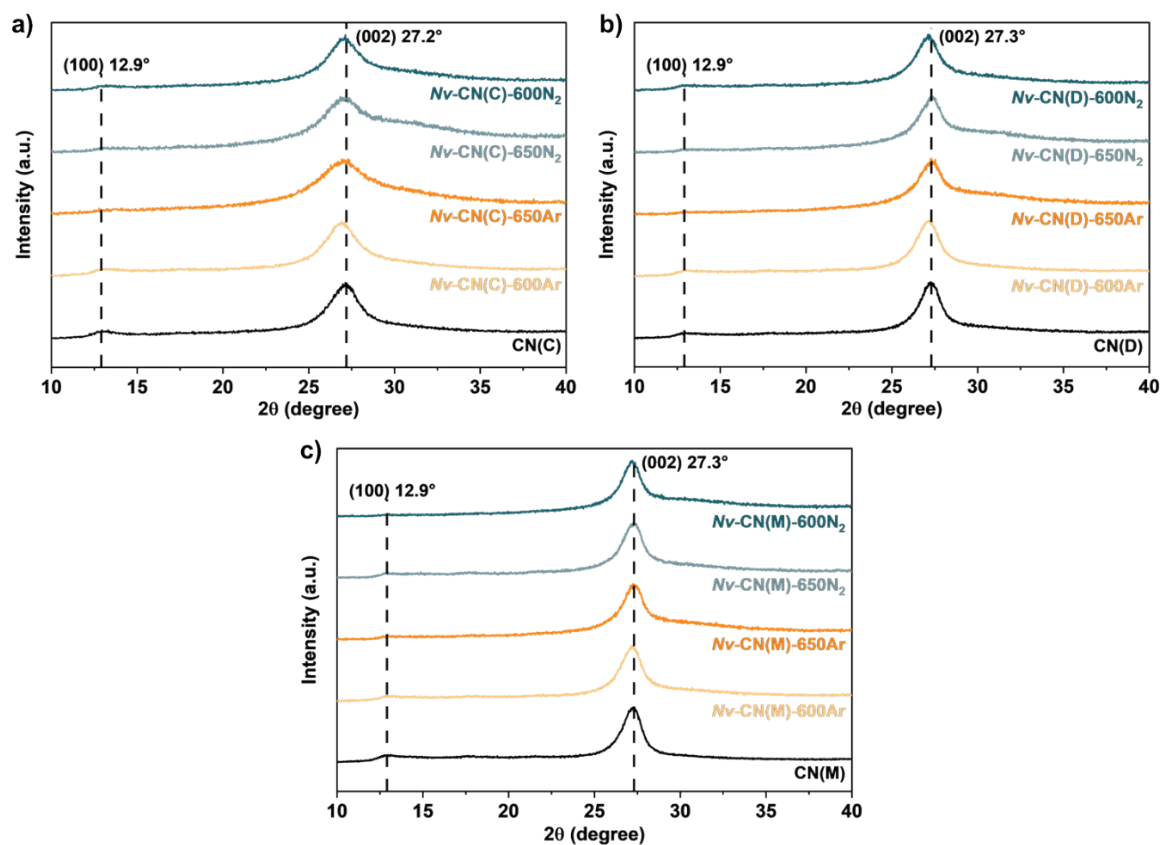


Figure S1. The XRD patterns of pristine and annealed CN derivatives using the precursor **a)** cyanamide, **b)** dicyandiamide, and **c)** melamine.

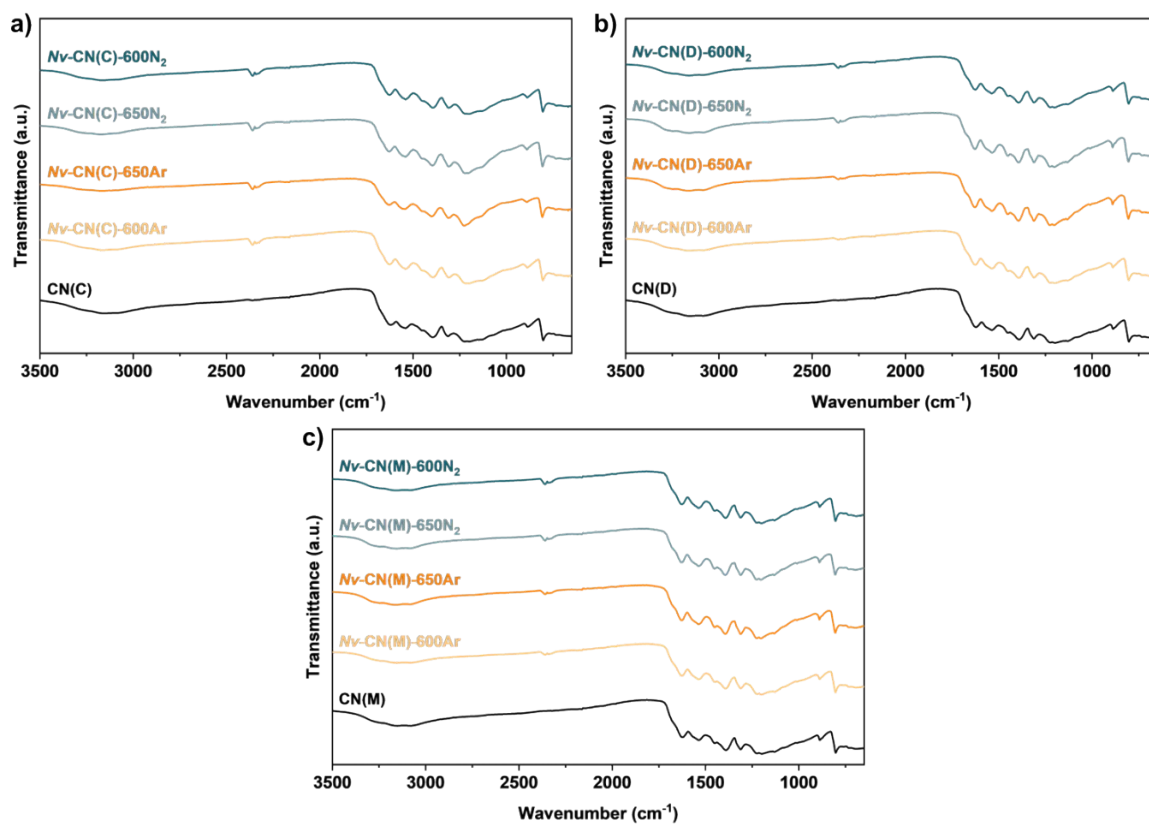


Figure S2. The FT-IR spectra of pristine and annealed CN derivatives using the precursor **a)** cyanamide, **b)** dicyandiamide, and **c)** melamine.

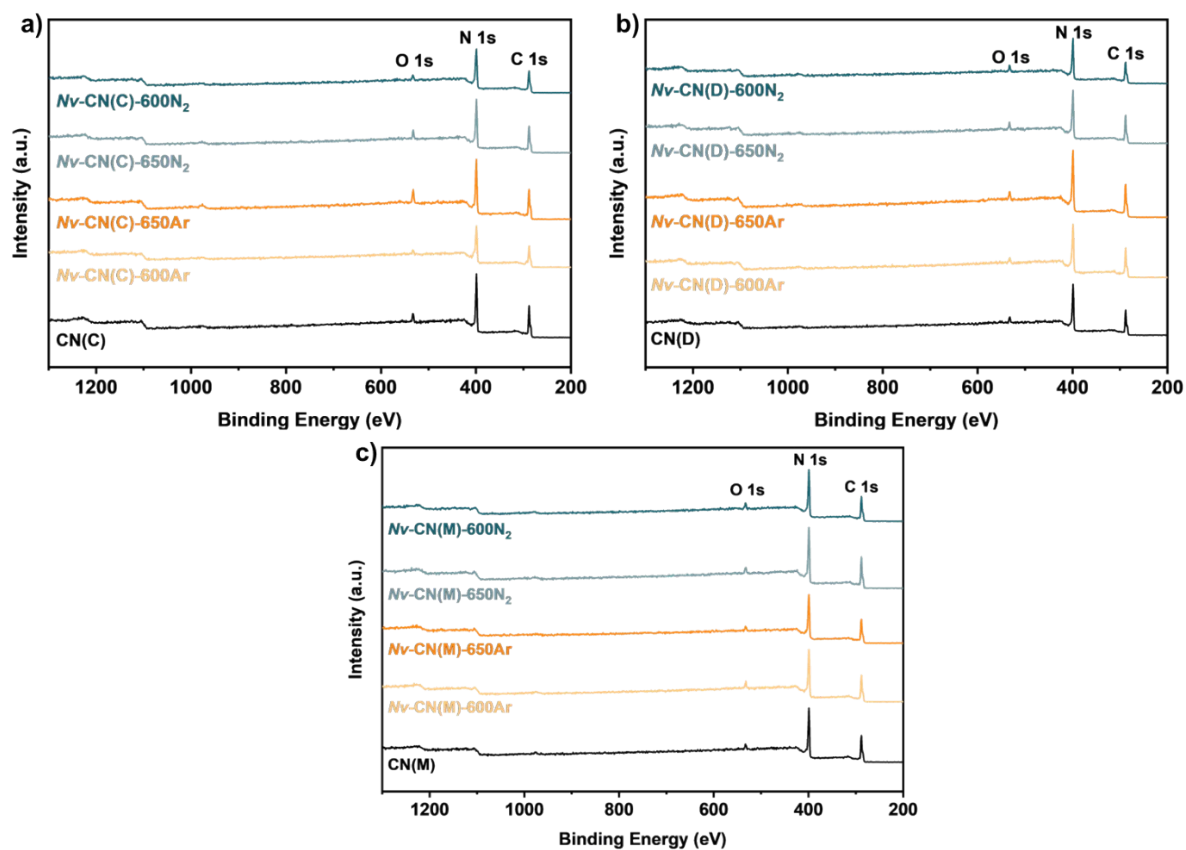


Figure S3. The XPS survey spectra of pristine and annealed CN derivatives using the precursor **a)** cyanamide, **b)** dicyandiamide, and **c)** melamine.

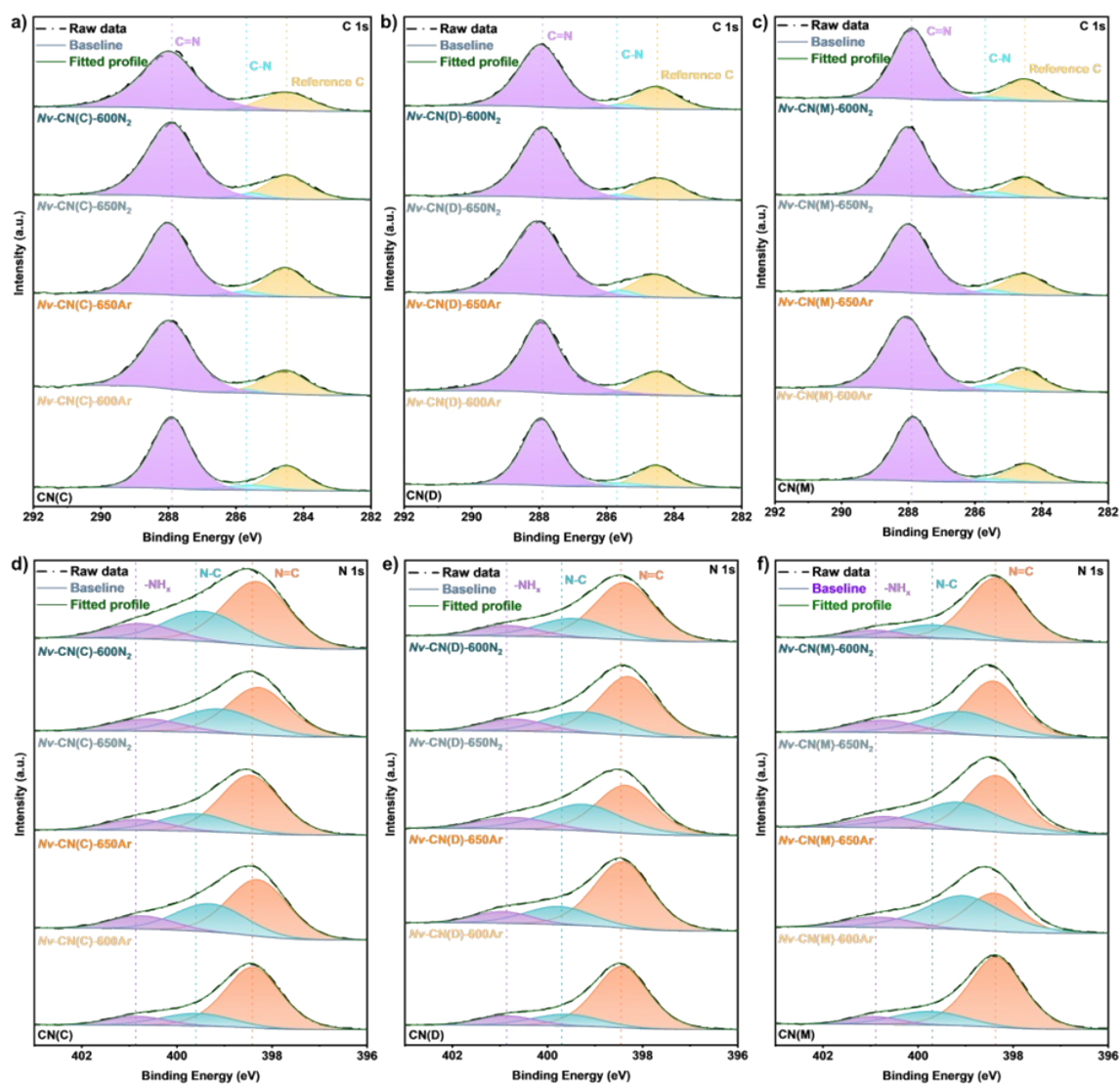


Figure S4. The high resolutions C 1s **a-c**) and N 1s **d-f**) XPS spectra of pristine and annealed CN derivatives using the precursor cyanamide, dicyandiamide, and melamine.

Table S1. Calculated C=N/–NH_x ratios of pristine and annealed CN derivatives by XPS peak area analysis.

Sample	Ratio	Sample	Ratio	Sample	Ratio
<i>CN(C)</i>	6.95	<i>CN(D)</i>	6.54	<i>CN(M)</i>	10.25
<i>Nv-CN(C)</i> 600N ₂	4.05	<i>Nv-CN(D)</i> 600N ₂	5.39	<i>Nv-CN(M)</i> 600N ₂	8.97
<i>Nv-CN(C)</i> 600Ar	4.15	<i>Nv-CN(D)</i> 600Ar	5.92	<i>Nv-CN(M)</i> 600Ar	5.29
<i>Nv-CN(C)</i> 650N ₂	3.46	<i>Nv-CN(D)</i> 650N ₂	4.62	<i>Nv-CN(M)</i> 650N ₂	3.68
<i>Nv-CN(C)</i> 650Ar	3.14	<i>Nv-CN(D)</i> 650Ar	3.48	<i>Nv-CN(M)</i> 650Ar	4.47

Table S2. Organic elemental composition (CHN) analysis of pristine and annealed CN derivatives.

Sample	C wt%	N wt%	H wt%	N/C ratio	Stoichiometry
<i>CN(C)</i>	33.78	61.47	1.76	1.56	$C_3N_{4.68}H_{1.85}$
<i>Nv</i> -CN(C)600N ₂	34.14	61.23	1.63	1.54	C ₃ N _{4.61} H _{1.70}
<i>Nv</i> -CN(C)600Ar	34.04	60.09	1.64	1.51	C ₃ N _{4.54} H _{1.72}
<i>Nv</i>-CN(C)650N₂	33.64	57.90	1.73	1.47	$C_3N_{4.43}H_{1.84}$
<i>Nv</i>-CN(C)650Ar	32.35	56.05	1.90	1.49	$C_3N_{4.47}H_{2.10}$
<i>CN(D)</i>	34.57	62.66	1.61	1.55	$C_3N_{4.66}H_{1.66}$
<i>Nv</i> -CN(D)600N ₂	34.29	61.51	1.60	1.54	C ₃ N _{4.61} H _{1.67}
<i>Nv</i> -CN(D)600Ar	34.41	61.99	1.57	1.54	C ₃ N _{4.63} H _{1.63}
<i>Nv</i> -CN(D)650N ₂	34.47	60.62	1.61	1.51	C ₃ N _{4.52} H _{1.67}
<i>Nv</i>-CN(D)650Ar	34.42	59.97	1.59	1.49	$C_3N_{4.48}H_{1.65}$
<i>CN(M)</i>	34.66	63.10	1.60	1.56	$C_3N_{4.68}H_{1.64}$
<i>Nv</i> -CN(M)600N ₂	34.56	61.80	1.55	1.53	C ₃ N _{4.60} H _{1.60}
<i>Nv</i> -CN(M)600Ar	34.46	61.20	1.55	1.54	C ₃ N _{4.57} H _{1.61}
<i>Nv</i> -CN(M)650N ₂	34.41	61.41	1.61	1.53	C ₃ N _{4.59} H _{1.67}
<i>Nv</i>-CN(M)650Ar	34.41	61.04	1.57	1.52	$C_3N_{4.56}H_{1.62}$

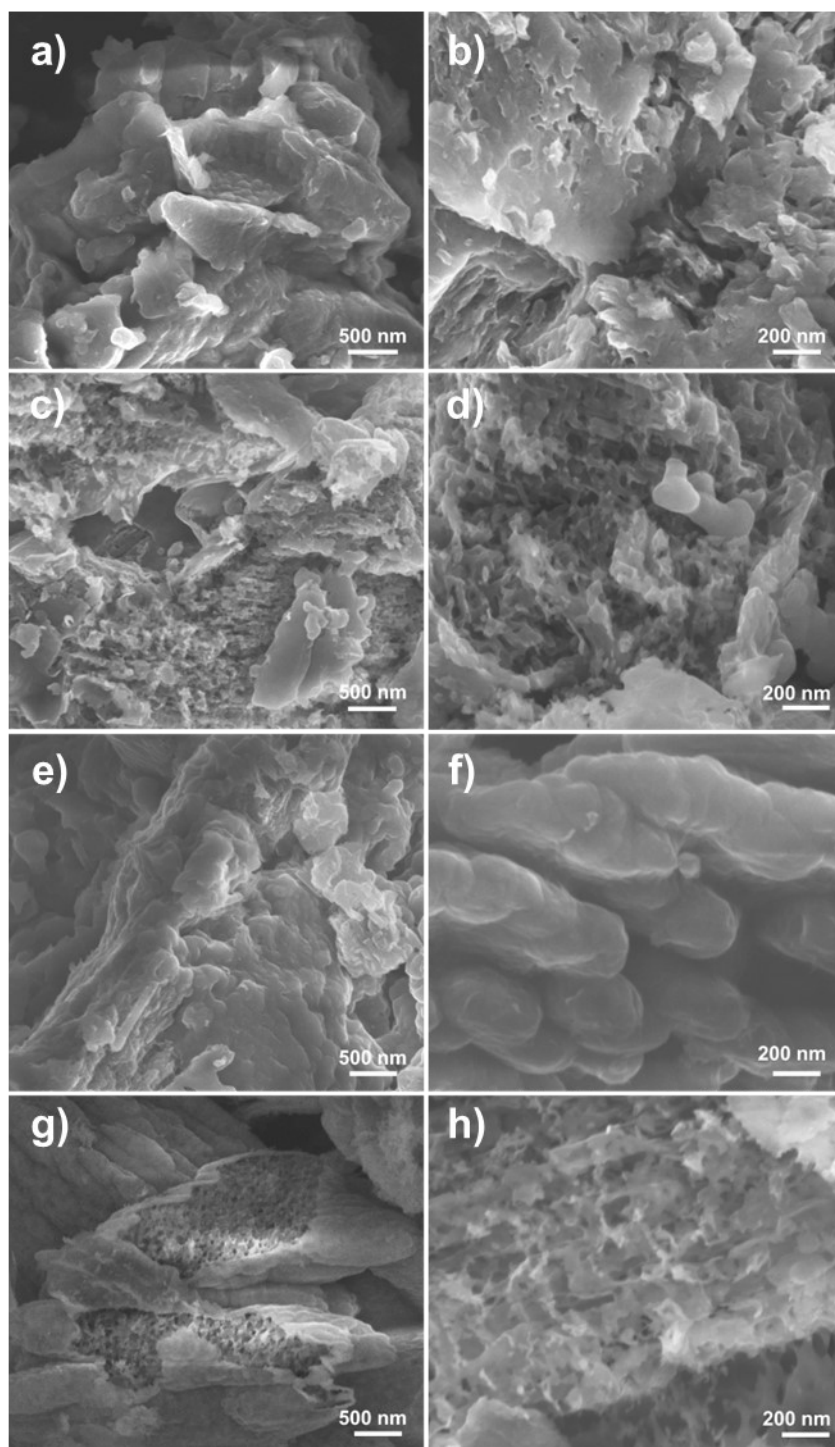


Figure S5. SEM images of **a** and **b**) CN(D), **c** and **d**) *Nv*-CN(D)600N₂, **e** and **f**) CN(M), **g** and **h**) *Nv*-CN(M)650Ar at different magnification.

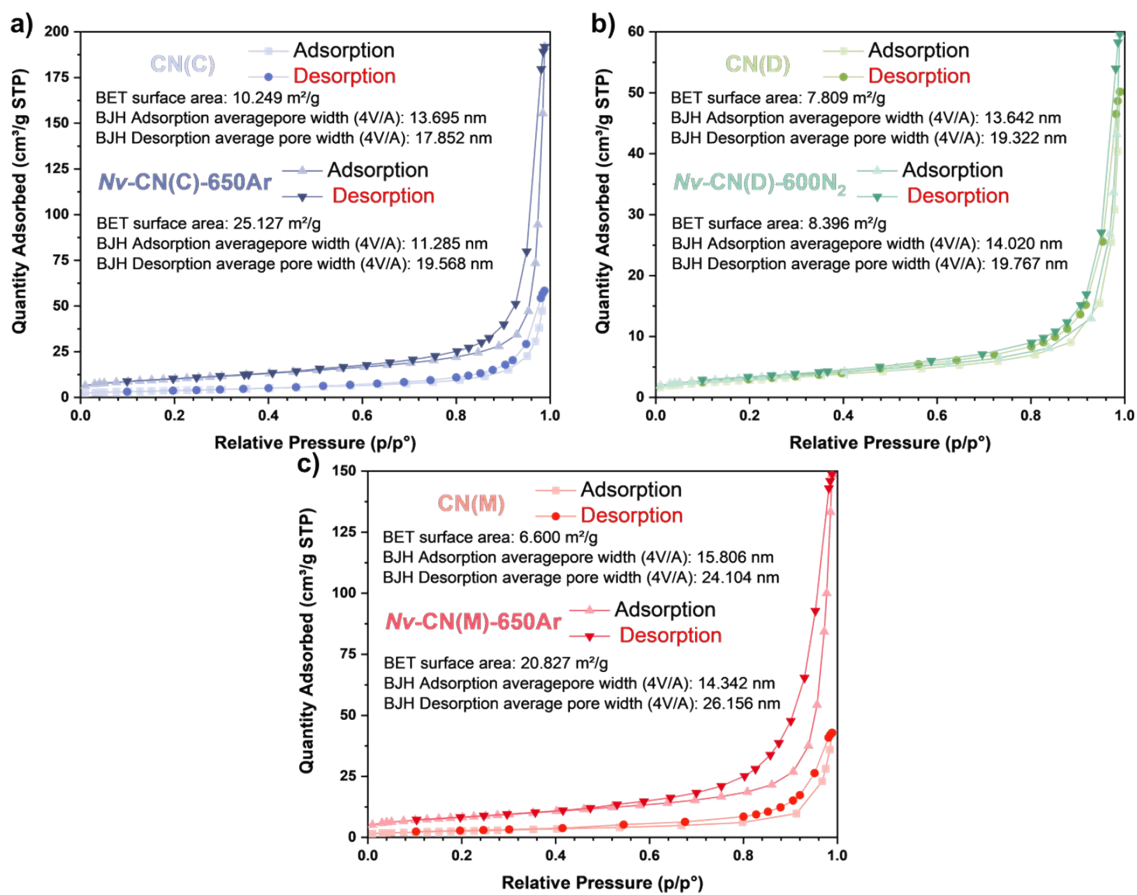


Figure S6. The Brunauer–Emmett–Teller (BET) N₂ adsorption/desorption isotherms of pristine and annealed CN derivatives using the precursor **a)** cyanamide, **b)** dicyandiamide, and **c)** melamine.

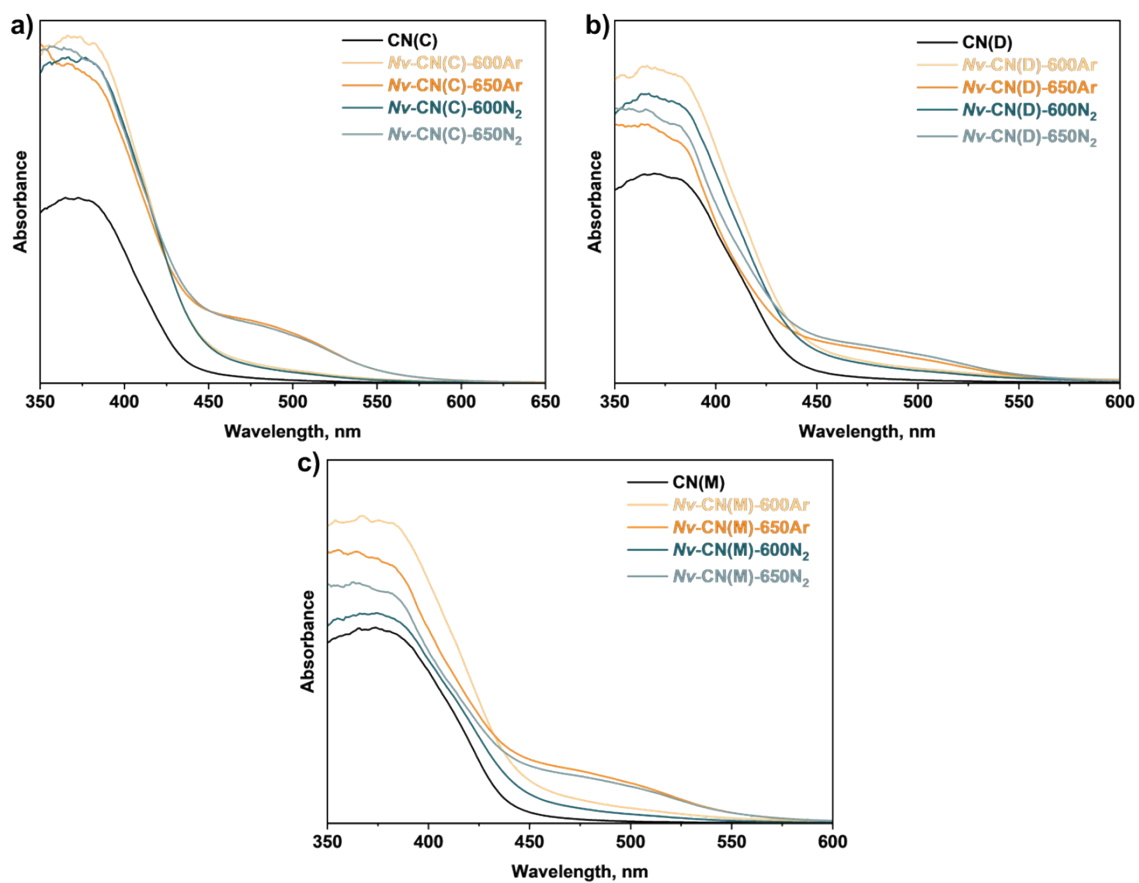


Figure S7. The UV-Vis absorption spectra of pristine and annealed CN derivatives using the precursor **a)** cyanamide, **b)** dicyandiamide, and **c)** melamine.

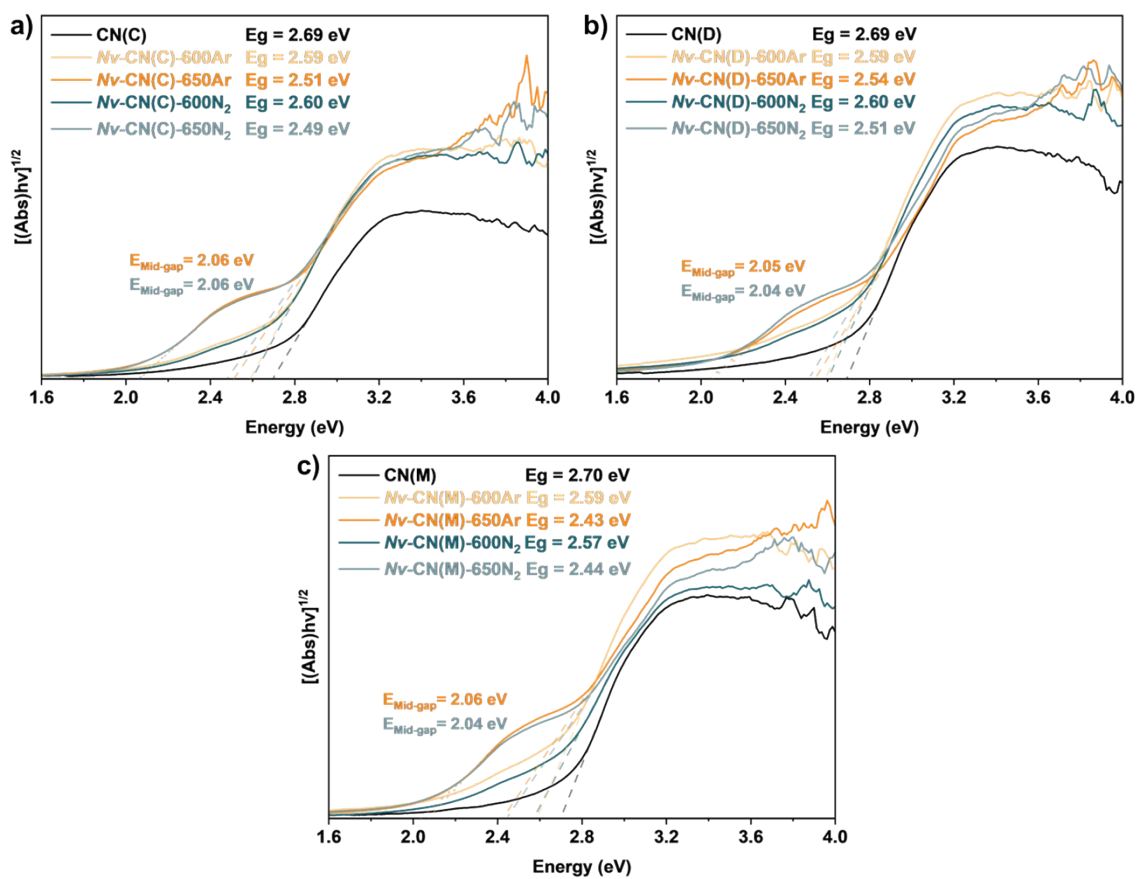


Figure S8. The Tauc plots of pristine and annealed CN derivatives using the precursor **a)** cyanamide, **b)** dicyandiamide, and **c)** melamine.

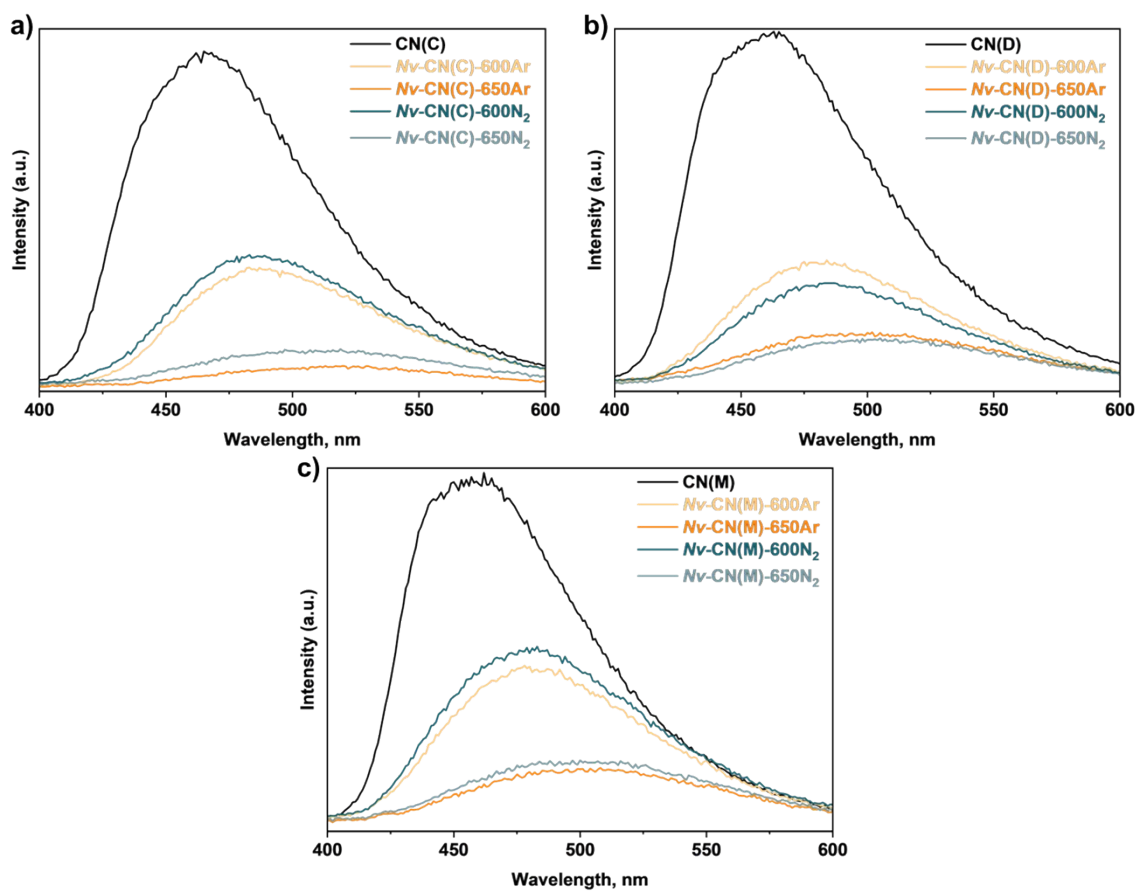


Figure S9. The PL spectra of pristine and annealed CN derivatives using the precursor **a)** cyanamide, **b)** dicyandiamide, and **c)** melamine.

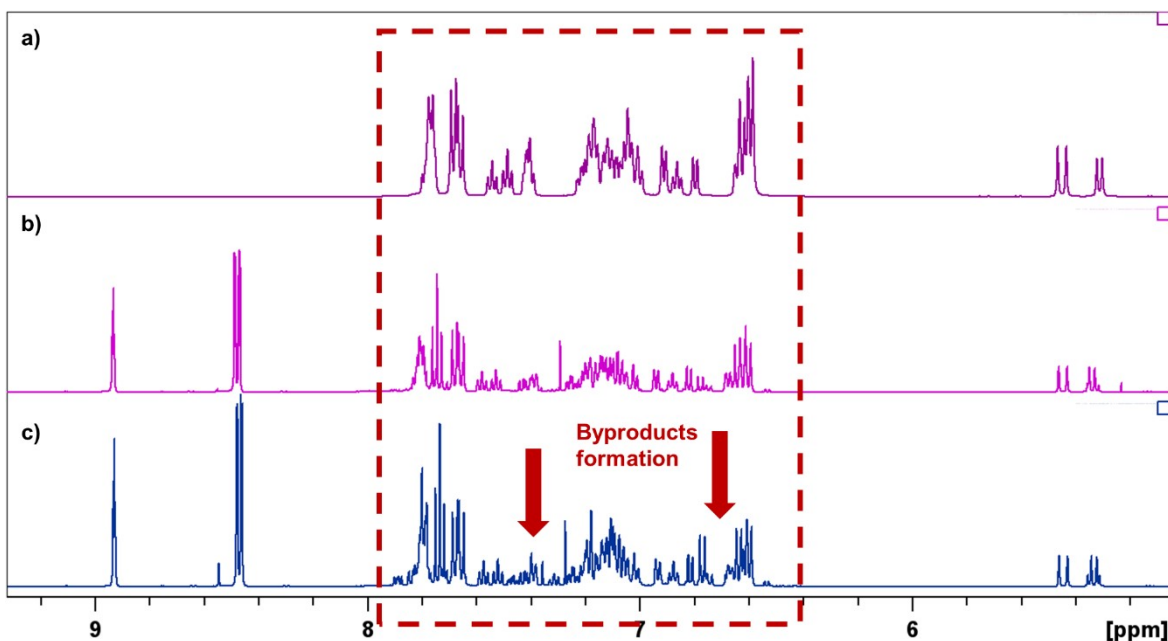


Figure S10. ^1H NMR of compound **5** a) pure, b) reaction time is 2 h and c) reaction time is 5 h (control experiments showing the possible degradation of compound **5** for longer period of reaction. Note* ^1H NMR in b) and c) contain internal standard 1,3-dinitrobenzene).

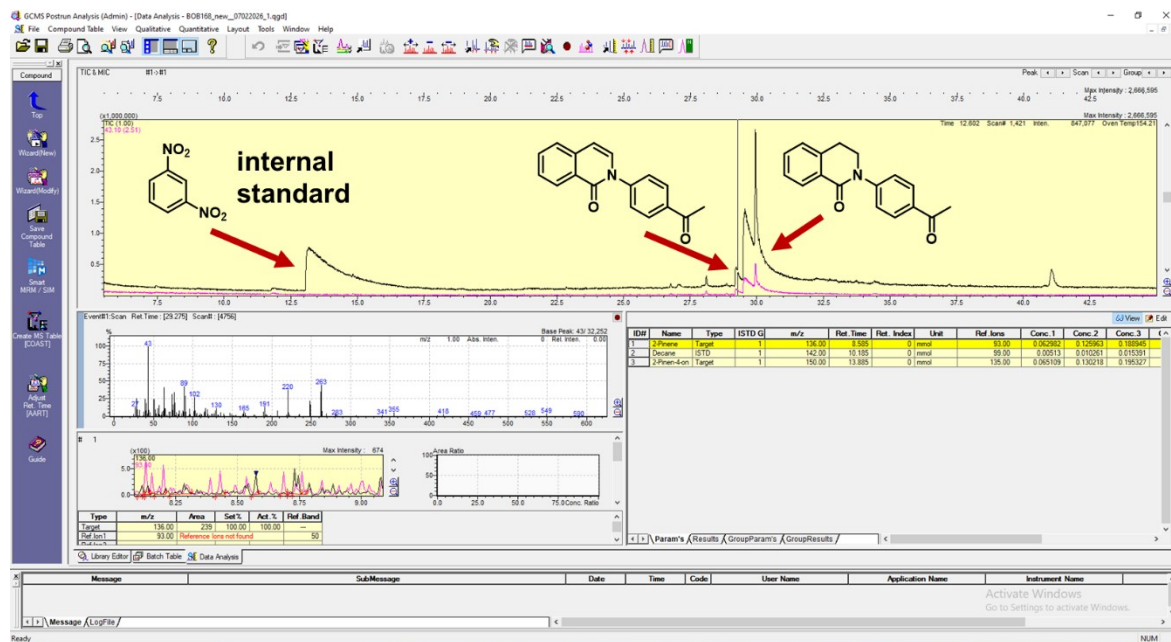


Figure S11. GC-MS of byproducts (compound **5** after treating under optimized conditions with longer duration).

Experimental procedure for degradation reaction: 0.03 mmol of purified compound **3** in 10 mL of 9:1 MeCN/DMSO mixture in the presence of 3 mg *Nv*-CN(C)-650Ar was irradiated with blue LED for 5 hours. At the end of the irradiation, 0.03 mmol of 1,3-dinitrobenzene was added to the mixture, then the mixture was filtrated through a syringe filter. After extraction of the filtrate with EtOAc, the organic phase was concentrated and then analyzed.

Table S3. Optimization table for the model reaction.

Entry	Photocatalyst	Catalyst Amount	Reaction Time	Solvent	Light Source	Yield% ^a
1	-	-	1h	1 mL MeCN	Low Mode Blue LED	14
2	CN(C)	3 mg	1h	1 mL MeCN	Low Mode Blue LED	20
3	<i>Nv</i> -CN(C)-600N ₂	3 mg	1h	1 mL MeCN	Low Mode Blue LED	27
4	<i>Nv</i> -CN(C)-600Ar	3 mg	1h	1 mL MeCN	Low Mode Blue LED	21
5	<i>Nv</i> -CN(C)-650N ₂	3 mg	1h	1 mL MeCN	Low Mode Blue LED	27
6	<i>Nv</i> -CN(C)-650Ar	3 mg	1h	1 mL MeCN	Low Mode Blue LED	30
7	CN(D)	3 mg	1h	1 mL MeCN	Low Mode Blue LED	15
8	<i>Nv</i> -CN(D)-600N ₂	3 mg	1h	1 mL MeCN	Low Mode Blue LED	25
9	<i>Nv</i> -CN(D)-	3 mg	1h	1 mL MeCN	Low	25

	600Ar				Mode Blue LED	
10	<i>Nv</i> -CN(D)- 650N ₂	3 mg	1h	1 mL MeCN	Low Mode Blue LED	24
11	<i>Nv</i> -CN(D)- 650Ar	3 mg	1h	1 mL MeCN	Low Mode Blue LED	20
12	CN(M)	3 mg	1h	1 mL MeCN	Low Mode Blue LED	14
13	<i>Nv</i> -CN(M)- 600N ₂	3 mg	1h	1 mL MeCN	Low Mode Blue LED	17
14	<i>Nv</i> -CN(M)- 600Ar	3 mg	1h	1 mL MeCN	Low Mode Blue LED	26
15	<i>Nv</i> -CN(M)- 650N ₂	3 mg	1h	1 mL MeCN	Low Mode Blue LED	26
16	<i>Nv</i> -CN(M)- 650Ar	3 mg	1h	1 mL MeCN	Low Mode Blue LED	27
17	<i>Nv</i> -CN(C)- 650Ar	3 mg	1h	5 mL MeCN	Low Mode Blue LED	37
18	<i>Nv</i> -CN(C)-	3 mg	1h	5 mL MeCN	High	70

	650Ar				Mode Blue LED	
19	<i>Nv</i> -CN(C)- 650Ar	5 mg	1h	5 mL MeCN	High Mode Blue LED	61
20	<i>Nv</i> -CN(C)- 650Ar	7 mg	1h	5 mL MeCN	High Mode Blue LED	65
21	<i>Nv</i> -CN(D)- 600N ₂	3 mg	1h	5 mL MeCN	Low Mode Blue LED	36
22	<i>Nv</i> -CN(D)- 600N ₂	3 mg	1h	5 mL MeCN	High Mode Blue LED	63
23	<i>Nv</i> -CN(M)- 650Ar	3 mg	1h	5 mL MeCN	Low Mode Blue LED	29
24	<i>Nv</i> -CN(M)- 650Ar	3 mg	1h	5 mL MeCN	High Mode Blue LED	51
25	<i>Nv</i> -CN(C)- 650Ar	3 mg	1h	5 mL Toluene	High Mode Blue LED	33
26	<i>Nv</i> -CN(C)- 650Ar	3 mg	1h	7 mL MeCN	High Mode Blue LED	68
27	<i>Nv</i> -CN(C)-	3 mg	1h	10 mL MeCN	High	76

	650Ar				Mode Blue LED	
28	<i>Nv</i> -CN(C)- 650Ar	3 mg	1h	10 mL (9:1) MeCN:DMF	High Mode Blue LED	57
29	<i>Nv</i> -CN(C)- 650Ar	3 mg	1h	10 mL (9:1) MeCN:THF	High Mode Blue LED	77
30	<i>Nv</i> -CN(C)- 650Ar	3 mg	1h	10 mL (9.5:0.5) MeCN:DMSO	High Mode Blue LED	73
31	<i>Nv</i> -CN(C)- 650Ar	3 mg	1h	10 mL (9:1) MeCN:DMSO	High Mode Blue LED	92
32	<i>Nv</i> -CN(C)- 650Ar	3 mg	1h	15 mL MeCN	High Mode Blue LED	62
33	<i>Nv</i> -CN(C)- 650Ar	3 mg	0.5h	10 mL (9:1) MeCN:DMSO	High Mode Blue LED	63
34	<i>Nv</i> -CN(C)- 650Ar	3 mg	2h	10 mL (9:1) MeCN:DMSO	High Mode Blue LED	73
35	<i>Nv</i> -CN(C)- 650Ar	3 mg	1h	10 mL (9:1) MeCN:DMSO	High Mode Cyan LED	44
36	<i>Nv</i> -CN(C)-	3 mg	1h	10 mL (9:1)	High	25

	650Ar			MeCN:DMSO	Mode Green LED	
37	<i>Nv</i> -CN(C)- 650Ar	3 mg	1h	10 mL (9:1) MeCN:DMSO	High Mode White LED	59
38	<i>Nv</i> -CN(C)- 650Ar	3 mg	1h	10 mL (9:1) MeCN:DMSO	DARK	0

^a0.25 mmol of **1** and **2** were used. Solvents were gassed with oxygen beforehand. Yields were determined by ¹H-NMR using 0.25 mmol 1,3-dinitrobenzene as the internal standard.

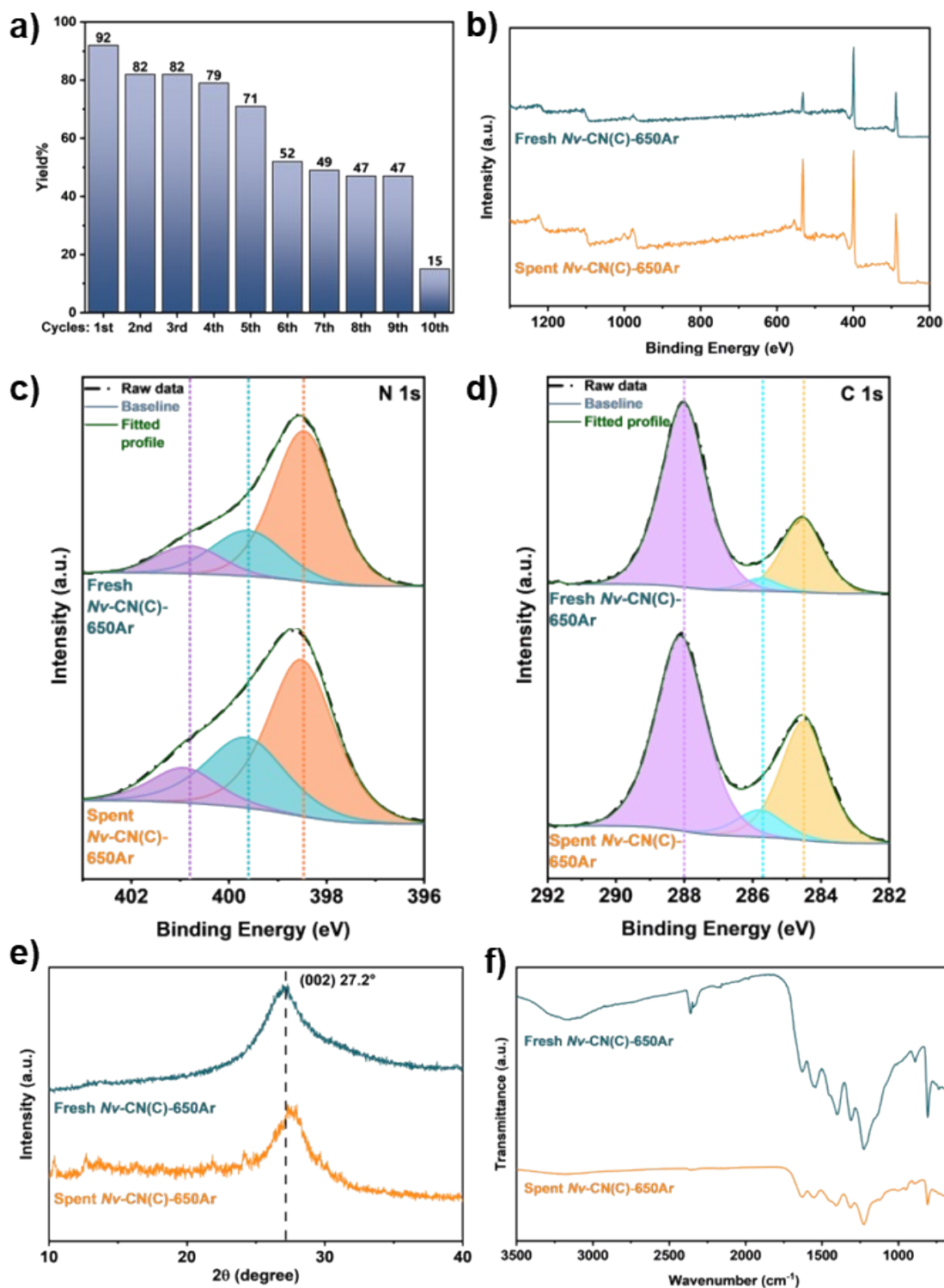


Figure S12. a) The reusability trials for ten consecutive cycles, b) The XPS survey spectra, The high resolutions c) C 1s and d) N 1s XPS spectra, e) The XRD pattern, and f) The FT-IR spectra of Nv-CN(C)-650Ar before and after use in ten consecutive cycles.

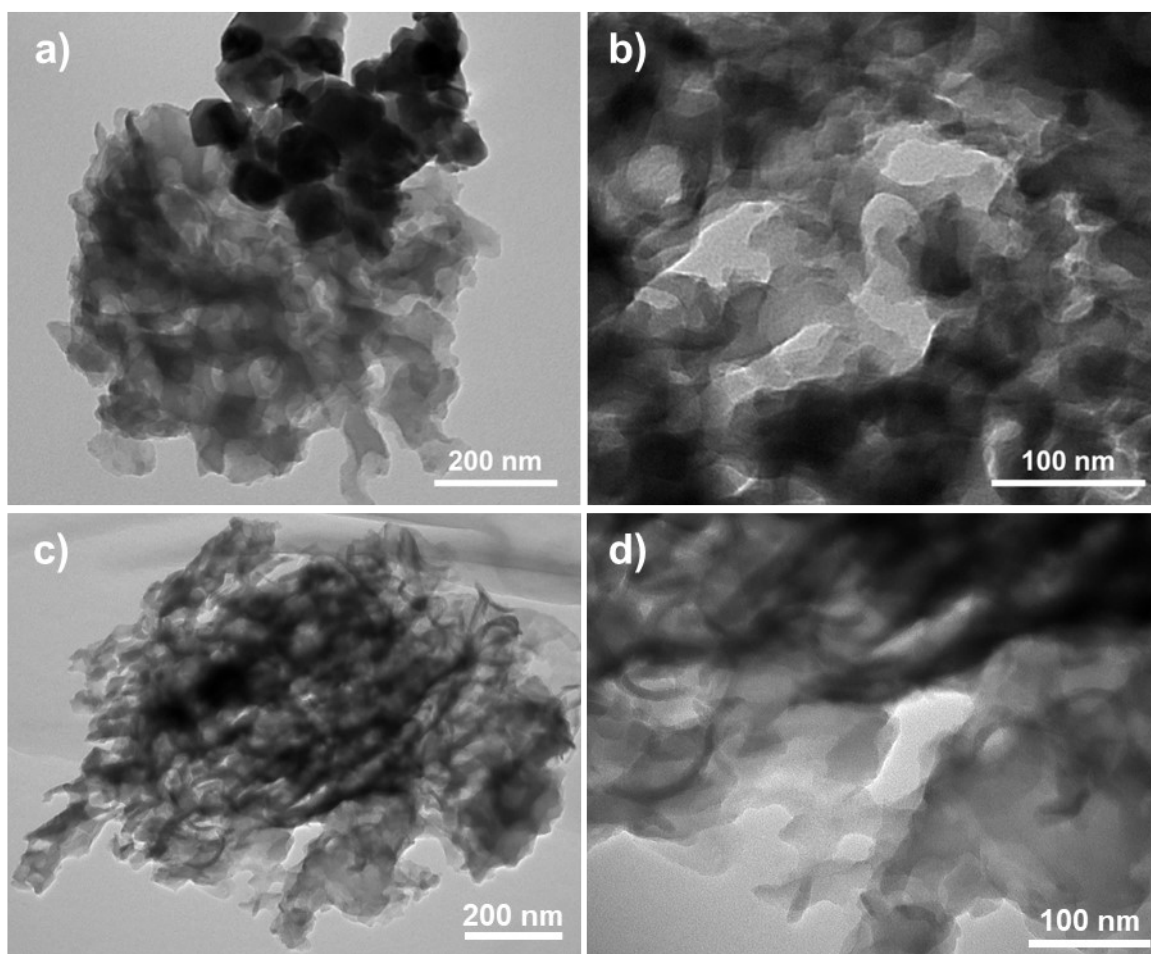
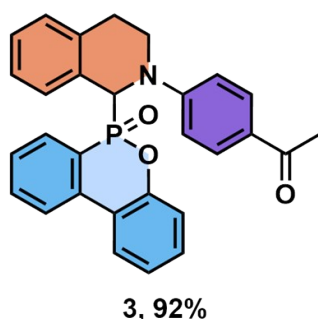


Figure S13. The TEM image of photocatalyst *Nv*-CN(C)-650Ar after **a-b**) five consecutive cycles of, and **c-d**) ten consecutive cycles of reusability experiments.

NMR Results



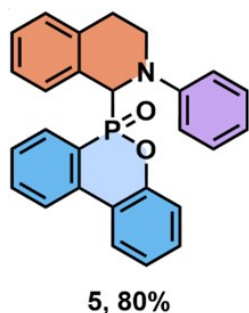
1-(4-(1-(6-oxidodibenzo[c,e][1,2]oxaphosphinin-6-yl)-3,4-dihydroisoquinolin-2(1H)-yl)phenyl)ethan-1-one (**3**), (92% yield, 1:3 d.r.)

^1H NMR (500 MHz, CDCl_3): δ 7.89-7.86 (m, 2H), 7.78 (d, $J=9.1$ Hz, 2H), 7.61-7.58 (m, 1H), 7.53-7.49 (m, 1H), 7.31-7.14 (m, 5H), 7.03 (d, $J=7.2$ Hz, 1H), 6.72-6.67 (m, 4H), 5.56 (d, $J=15.50$ Hz, 1H), 3.38-3.33 (m, 1H), 3.31-3.25 (m, 1H), 2.75-2.70 (m, 1H), 2.51-2.44 (m, 1H), 2.50 (s, 3H).

^{13}C NMR (125.7 MHz, CDCl_3): 196.52, 151.96, 151.67, 149.69, 136.85, 135.70, 135.66, 133.94, 132.17, 130.52, 130.10, 128.75, 128.30, 128.21, 128.10, 127.98, 127.17, 126.80, 124.71, 124.43, 123.21, 123.13, 119.66, 119.61, 112.66, 61.46, 42.94, 27.17, 26.11.

^{31}P NMR (202.4 MHz, CDCl_3): δ 31.82, 31.47.

6-(2-phenyl-1,2,3,4-tetrahydroisoquinolin-1-yl)dibenzo[c,e][1,2]oxaphosphinine 6-oxide (**5**), (80% yield, 1:3 d.r.)

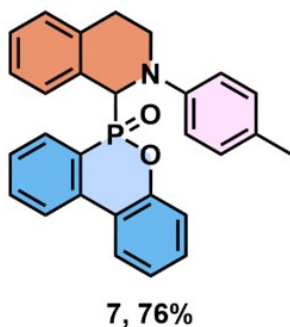


^1H NMR (500 MHz, CDCl_3): δ 7.88-7.85 (m, 2H), 7.59-7.55 (m, 2H), 7.31-7.10 (m, 6H), 7.00 (d, $J=7.30$ Hz, 1H), 6.78-6.72 (m, 4H), 6.68 (d, $J=8.43$ Hz, 2H), 5.42 (d, $J=17.56$ Hz, 1H), 3.38-3.33 (m, 1H), 3.22-3.18 (m, 1H), 2.72-2.66 (m, 1H), 2.36-2.31 (m, 1H).

^{13}C NMR (125.7 MHz, CDCl_3): 150.05, 149.98, 148.70, 148.67, 136.79, 136.24, 133.57, 132.25, 132.18, 130.23, 129.00, 128.85, 128.46, 128.04, 128.00, 127.98, 127.89, 127.73, 127.70, 126.46, 126.44, 124.57, 124.06, 123.04, 62.06, 44.43, 26.79.

^{31}P NMR (202.4 MHz, CDCl_3): δ 33.14, 32.05.

6-(2-(p-tolyl)-1,2,3,4-tetrahydroisoquinolin-1-yl)dibenzo[c,e][1,2]oxaphosphinine 6-oxide (**7**), (76% yield, 1:6 d.r.)



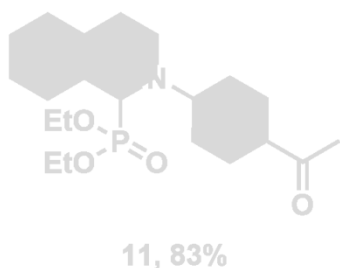
^1H NMR (500 MHz, CDCl_3): δ 7.90-7.87 (m, 2H), 7.61-7.55 (m, 2H), 7.42-7.38 (m, 1H), 7.28-7.15 (m, 6H), 7.01 (d, $J=7.45$ Hz, 1H), 6.93 (d, $J=8.50$ Hz, 2H), 6.86 (dd, $J=7.66$ Hz, $J=1.67$ Hz, 2H), 5.32 (d, $J=18.27$ Hz, 1H), 3.41-3.36 (m, 1H), 3.21-3.16 (m, 1H), 2.71-2.67 (m, 1H), 2.36-2.30 (m, 1H), 2.21 (s, 3H).

^{13}C NMR (125.7 MHz, CDCl_3): 150.12, 146.49, 140.52, 138.27, 136.07, 131.92, 130.84, 130.26,

130.12, 129.75, 129.53, 129.38, 128.70, 128.05, 127.14, 125.19, 124.61, 124.29, 124.03, 120.69, 120.38, 119.86, 116.63, 115.65, 62.30, 44.04, 28.61, 20.27.

^{31}P NMR (202.4 MHz, CDCl_3): δ 33.25, 31.73.

diethyl (2-(4-acetylphenyl)-1,2,3,4-tetrahydroisoquinolin-1-yl)phosphonate (11),
(83% yield)

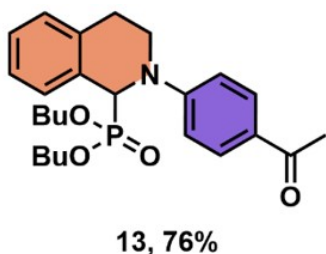


^1H NMR (500 MHz, CDCl_3): δ 7.89 (d, $J = 9.05$ Hz, 2H), 7.36 (d, $J = 9.05$ Hz, 1H), 7.24-7.18 (m, 3H), 6.96 (d, $J = 9.05$ Hz, 2H), 5.32 (d, $J = 17.95$ Hz 1H), 4.13 (q, $J = 7.05$ Hz 4H), 3.86-3.80 (m, 1H), 3.68-3.63 (m, 1H), 3.35-3.29 (m, 1H), 3.04-2.98 (m, 1H), 2.46 (s, 3H), 1.26 (t, $J = 7.07$ Hz 6H).

^{13}C NMR (125.7 MHz, CDCl_3): 196.47, 152.68, 137.41, 136.34, 134.39, 130.31, 129.08, 128.52, 128.09, 127.93, 126.94, 126.21, 124.58, 63.29, 58.59, 43.39, 29.67, 27.44, 16.43.

^{31}P NMR (202.4 MHz, CDCl_3): δ 21.32.

dibutyl (2-(4-acetylphenyl)-1,2,3,4-tetrahydroisoquinolin-1-yl)phosphonate (13),
(76% yield)

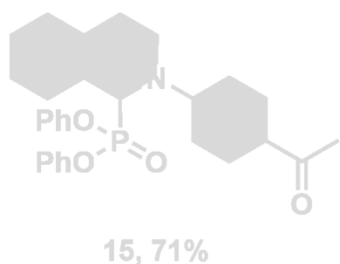


^1H NMR (500 MHz, CDCl_3): δ 7.84 (d, $J = 9.05$ Hz, 2H), 7.30 (d, $J = 7.45$ Hz, 1H), 7.25-7.16 (m, 3H), 6.88 (d, $J = 8.96$ Hz, 2H), 5.26 (d, $J = 18.06$ Hz 1H), 3.99-3.86 (m, 3H), 3.83-3.76 (m, 1H), 3.71-3.59 (m, 2H), 3.29-3.23 (m, 1H), 2.99-2.93 (m, 1H), 2.44 (s, 3H), 1.51-1.45 (m, 2H), 1.40-1.35 (m, 2H), 1.26-1.11 (m, 4H), 0.81 (t, $J = 7.35$ Hz 3H), 0.75 (t, $J = 7.44$ Hz 3H).

^{13}C NMR (125.7 MHz, CDCl_3): 197.11, 164.15, 147.20, 138.23, 134.33, 132.43, 130.36, 129.38, 128.89, 127.45, 127.02, 124.57, 112.30, 66.89, 58.51, 57.25, 43.33, 32.48, 29.67, 27.47, 26.74, 18.61, 18.57, 13.53, 13.48.

^{31}P NMR (202.4 MHz, CDCl_3): δ 21.46.

diphenyl (2-(4-acetylphenyl)-1,2,3,4-tetrahydroisoquinolin-1-yl)phosphonate (15)
(71% yield)



^1H NMR (500 MHz, CDCl_3): δ 7.93 (d, $J = 9.01$ Hz, 2H), 7.51-7.49 (m, 1H), 7.32-7.22 (m, 5H), 7.17-7.11 (m, 3H), 7.07-7.03 (m, 3H), 6.97 (d, $J = 8.53$ Hz, 2H), 6.82 (d, $J = 8.53$ Hz, 2H), 5.76 (d, $J = 17.62$ Hz 1H), 4.06-4.01 (m, 1H), 3.74-3.69 (m, 1H), 3.34-3.30 (m, 1H), 3.08-3.03 (m, 1H), 2.53 (s, 3H).

^{13}C NMR (125.7 MHz, CDCl_3): 196.49, 152.08, 150.46, 150.37, 150.17, 150.08, 136.40, 136.35, 130.45, 129.66, 129.52, 129.29, 128.79, 128.45, 128.42, 128.36, 128.31, 127.45, 126.55, 126.53, 125.22, 125.03, 120.46, 120.12, 112.74, 59.03, 43.61, 29.67, 27.37.

^{31}P NMR (202.4 MHz, CDCl_3): δ 13.81.

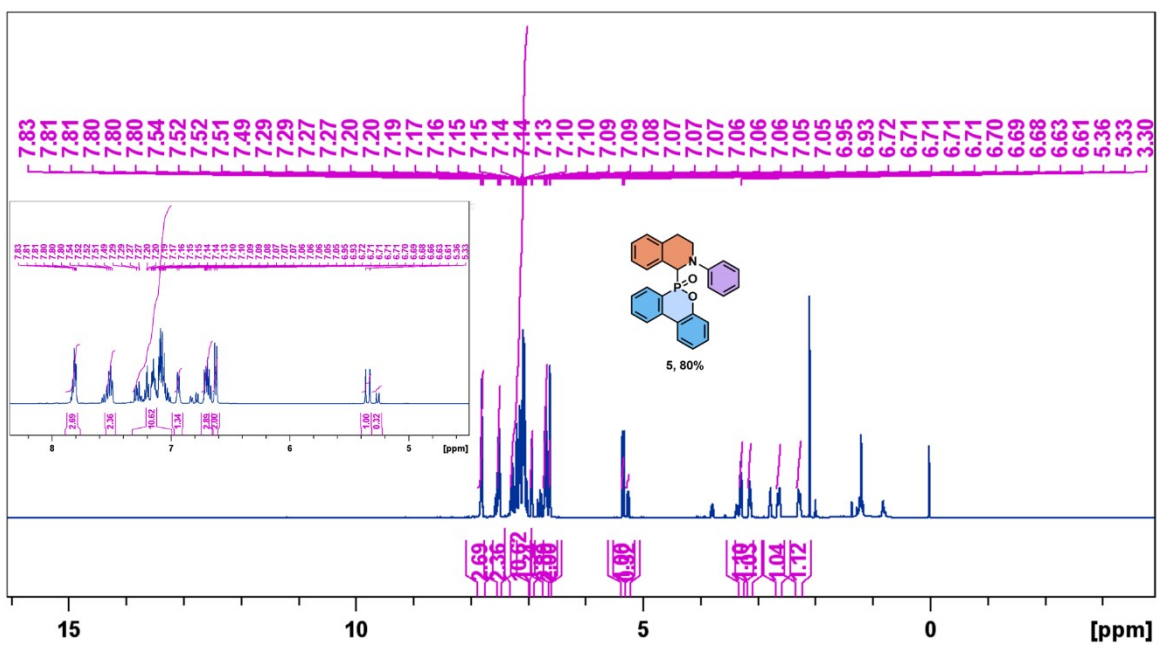


Figure S16. ¹H NMR of compound 5 (CDCl₃).

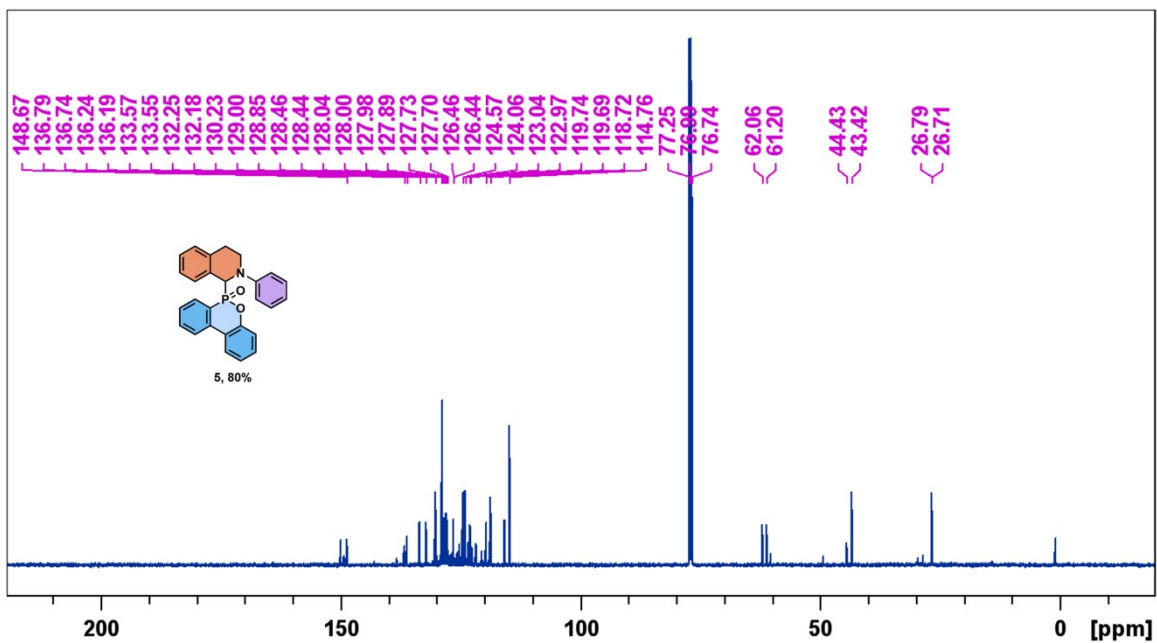


Figure S17. ¹³C NMR of compound 5 (CDCl₃).

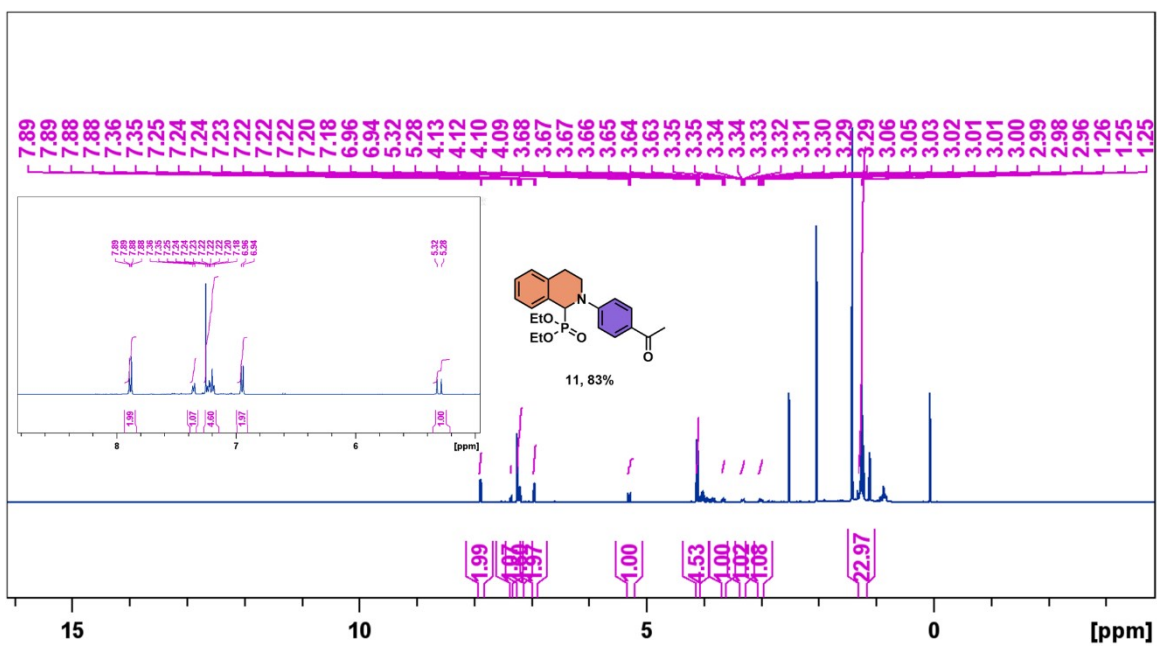


Figure S20. ¹H NMR of compound 11 (CDCl₃).

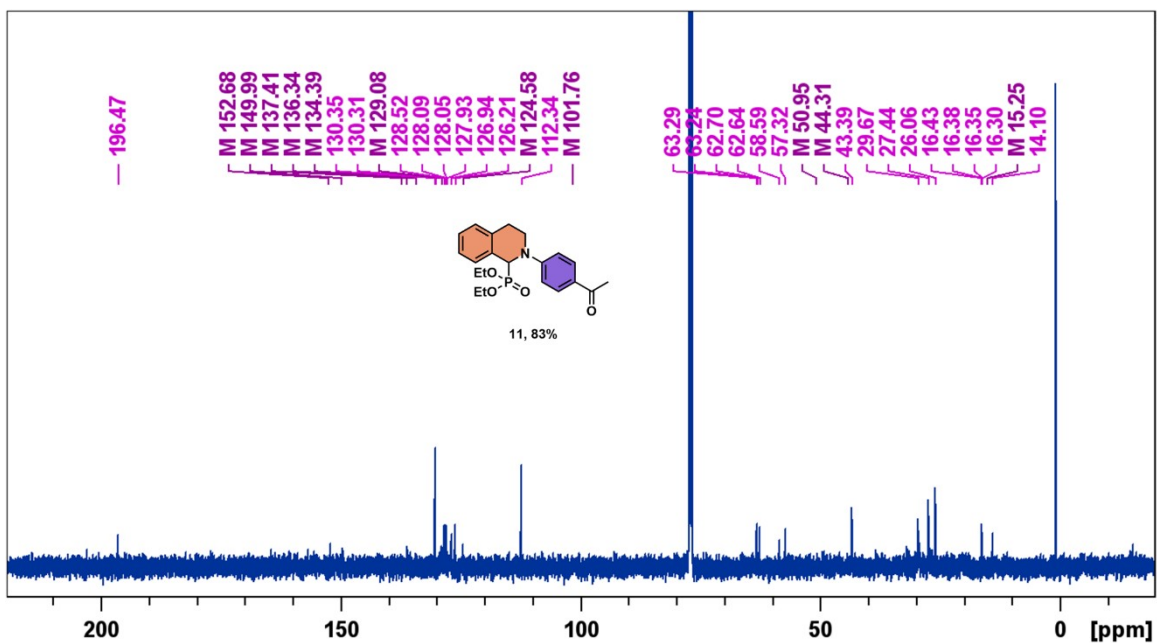


Figure S21. ¹³C NMR of compound 11 (CDCl₃).

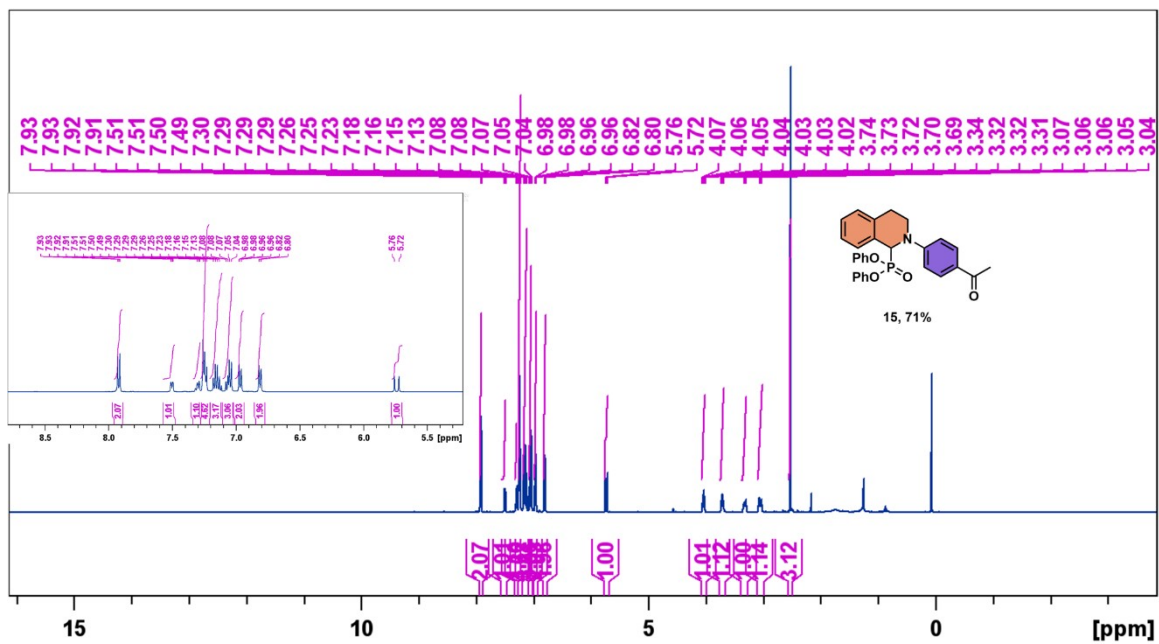


Figure S24. ¹H NMR of compound 15 (CDCl₃).

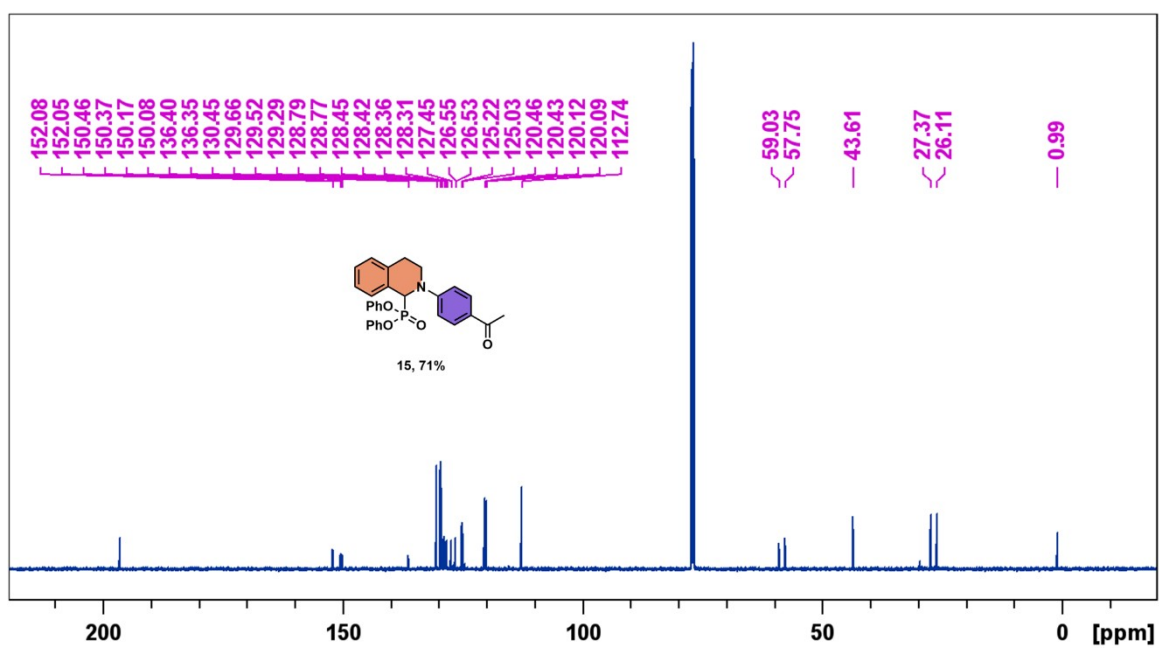


Figure S25. ¹³C NMR of compound 15 (CDCl₃).

References

- 1 F. Y. Kwong, A. Klapars and S. L. Buchwald, *Org Lett*, 2002, **4**, 581–584.